analytical chemistry

pubs.acs.org/ac Article

Normalization of Samples of Limited Amounts in Quantitative Metabolomics Using Liquid Chromatography Fluorescence Detection with Dansyl Labeling of Metabolites

Xian Luo,[†] Yiman Wu,[†] and Liang Li*

Cite This: *Anal. Chem.* 2021, 93, 3418−3425 Read Online

ACCESS | Metrics & More | Article Recommendations | Supporting Information

ABSTRACT: Quantitative metabolomics requires the analysis of the same or a very similar amount of samples in order to accurately determine the concentration differences of individual metabolites in comparative samples. Ideally, the total amount or concentration of metabolites in each sample is measured to normalize all the analyzed samples. In this work, we describe a very sensitive method to measure a subclass of metabolites as a surrogate quantifier for normalization of samples with limited amounts. This method starts with low-volume dansyl labeling of all metabolites containing a primary/secondary amine or phenol group in a sample to produce a final solution of 21 μL. The dansyl-labeled metabolites generate fluorescence signals at 520 nm with photoexcitation at 250 nm. To remove the interference of dansyl hydroxyl products (Dns-OH) formed from the labeling reagents used, a fast-gradient liquid chromatography separation is used to elute Dns-OH using aqueous solution, followed by organic solvent elution to produce a chromatographic peak of labeled metabolites, giving a measurement throughput of 6 min per sample. The integrated fluorescence signals of the peak are found to be related to the injection amount of the dansyl-labeled metabolites. A calibration curve using mixtures of dansyl-labeled amino acids is used to determine the total concentration of labeled metabolites in a sample. This concentration is used for normalization of samples in the range from 2 to 120 μM in 21 μL with only 1 μL consumed for fluorescence quantification (i.e., 2−120 pmol). We demonstrate the application of this sensitive sample normalization method in comparative metabolome analysis of human cancer cells, MCF-7 cells, treated with and without resveratrol, using a starting material of as low as 500 cells.

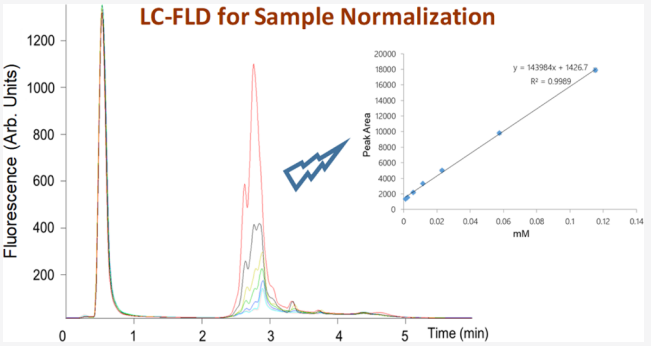

INTRODUCTION

Quantitative metabolomics uses analytical platforms to detect and quantify a large fraction of the metabolome in biological samples. Among different analytical platforms employed in metabolomics, liquid chromatography−mass spectrometry (LC−MS) provides relatively high sensitivity.[1] In particular, using high-performance chemical isotope labeling (CIL) of metabolites to concomitantly improve separation and enhance ionization, a very high coverage of the metabolome can be attained.[2] In addition, using differential CIL to label individual samples with a light reagent and a pooled or control sample with a heavy reagent allows accurate relative quantification of individual metabolites.[2−8]

While CIL LC−MS improves coverage and accuracy, the overall quantification accuracy is also dependent on how the starting materials are handled. Variations in the total concentration of metabolites among different samples need to be strictly controlled in order to determine the concentration differences of individual metabolites in comparative samples.[9] In other words, sample amount or concentration normalization is often required, especially for samples with inherently large concentration differences such as urine, cell extracts of different cells or cell numbers, and tissues of different sizes or cell densities.[9] In addition, knowing the concentration of each sample, we can inject the same amount of individual samples to eliminate the detection bias associated with injection amount variations.[10] For the latter, injecting the same volume of a dilute sample, compared to that of a concentrated sample, would reduce the chance of detecting the low abundance metabolites, as their signals would be below the detection limit. This problem can be addressed by normalizing the concentration of all individual samples and then injecting the same volume (i.e., injecting the same amount).

In our previous work, we reported an LC-UV-based sample normalization method where the amine- or phenol-containing

Received: October 25, 2020
Accepted: January 21, 2021
Published: February 8, 2021

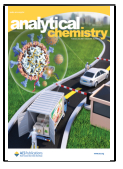

https://dx.doi.org/10.1021/acs.analchem.0c04508
Anal. Chem. 2021, 93, 3418−3425

metabolites are labeled using dansyl chloride, followed by LC-UV quantification of the labeled metabolites.[11] This method has been widely used for normalization of many different types of samples.[12−17] However, it requires the injection of 5 μL of the sample with a minimum concentration of 20 μM or a minimum sample amount of 100 pmol. While this sensitivity is sufficient for handling most metabolomics samples, it is not adequate for quantifying samples of limited amounts such as analyzing the metabolome of small numbers of cells.[18−22]

In this work, we explored the fluorescence characteristics of dansyl-labeled metabolites and developed a method using fast LC with a fluorescence detector (FLD) to quantify the total concentration of metabolites in samples of limited amounts. We illustrated the application of this method for sample normalization of cell lysates with a starting material of 500−10,000 MCF-7 cancer cells. We showed much improved relative quantification of metabolites in two comparative groups of samples by reducing intragroup data variation and increasing intergroup data separation after sample normalization. To our knowledge, there is no report of any other methods that can normalize samples of these low quantities. For the first time, we demonstrate the suitability of LC-FLD, using a conventional and commercially available equipment, for the purpose of sample normalization. Moreover, we show that this method can be used to normalize samples in the range of 2−120 pmol, which is compatible with high-coverage metabolome analysis using CIL nanoLC−MS. We envisage the integration of LC-FLD sample normalization with CIL nanoLC−MS for high-coverage quantitative metabolomics of small numbers of cells and other types of samples with a limited amount of starting materials.

EXPERIMENTAL SECTION

Cell Culture and Processing. MCF-7 breast cancer cell (ATCC HTB-22) was cultured in a Hyclone DMEM medium (Logan, UT) supplemented with 10% Gibco FBS (Grand Island, NY) in a humidified incubator at 37 °C with 5% carbon dioxide supplied. Details of cell culture and processing are shown in Note S1.

Resveratrol Treatment Experiment. Figure S1 shows the workflow for biological triplicate experiments ($n = 3$) of each cell group. For the resveratrol-treatment group, when the MCF-7 cell culture confluence reached 80%, the growth medium was replaced with 50 μM resveratrol prepared by dissolving resveratrol in dimethyl sulfoxide (DMSO) and then diluted with serum-free Dulbecco's modified Eagle's medium (DMEM). The final concentration of DMSO in DMEM was less than 0.01% (v/v). For the control group, the growth medium was replaced with the same concentration of DMSO in DMEM. The two groups of cells were incubated at 37 °C for 24 h before harvesting. About 1000 and 2000 cells were harvested and aliquoted into separate vials for further processing.

Sample Preparation and Chemical Isotope Labeling. The cells were lysed by freeze−thaw cycles and extracted with 50% methanol in water. Briefly, 50 μL of 50% methanol in water (v/v) was added into vials, and the vials were placed in liquid nitrogen for 1 min and thawed on an ice-water bath for 1 min. This procedure was repeated four more times. The cell lysates were centrifuged at 16,000*g* at 4 °C for 10 min to remove the cell debris, and the supernatant was transferred into another vial and dried down in a Savant SC110A SpeedVac. The lysates were labeled using dansyl chloride (DnsCl) (Note S1).[23] Each individual sample was labeled using ^{12}C-DnsCl in experimental triplicates. A ^{13}C-labeled pooled sample used as a reference was prepared by mixing equal volumes of multiple samples (36 vials of 1000-cell lysates and 36-vials of 2000-cell lysate) separately labeled using ^{13}C-DnsCl before normalization. We used small numbers of cells for preparing the pooled sample in order to maintain a similar matrix effect on labeling the reference sample and the individual samples. In this way, for a metabolite with a similar concentration in the pooled sample and an individual sample, the intensity ratio of the ^{13}C-labeled metabolite in the pooled sample and the ^{12}C-labeled metabolite in an individual sample will be close to 1:1, which can facilitate the data analysis such as in peak-ratio-based peak pair picking, peak pair filtering, and so forth.[24] We note that even if the extent of the matrix effect on labeling the reference sample is different from those of individual samples, it will not affect the relative quantification of metabolites in individual samples, as the individual samples (e.g., all 1000-cell samples) have similar matrices and thus labeling efficiencies.[25] The labeled samples and pool were separately injected into LC-FLD for determining the total concentration of the labeled metabolites. The ^{12}C-labeled individual sample and the ^{13}C-labeled pool were mixed in equal mole based on the LC-FLD quantification results and dried down in a SpeedVac. The mixture was redissolved by 9:1 (v/v) H_2O/ACN and injected into nanoLC−MS for metabolite detection (see Results and Discussion).

LC-FLD. An Agilent 1220 Infinity II LC system (Santa Clara, CA) with an FLD was used for quantification. One microliter of labeled lysates was injected onto an Agilent Poreshell 120 EC-C18 column (2.1 × 30 mm, 2.7 μm). Solvent A was 0.1% (v/v) formic acid and 5% (v/v) acetonitrile in water, and solvent B was 0.1% (v/v) formic acid in acetonitrile. The LC conditions were as follows: $t = 0$, 0% B; t =0.5 min, 0% B %; $t = 0.51$ min, 100% B; $t = 2.5$ min, 100% B; $t = 2.51$ min 0% B; and $t = 6$ min, 0% B. The flow rate was 0.45 mL/min. The excitation wavelength was 250 nm, and the emission wavelength was 520 nm. The gain of the detector was set at 18.

nanoLC−MS. The LC−MS platform was Waters nano-Acquity UPLC (Milford, MA) linked to the Bruker Impact HD Q-TOF mass spectrometer (Billerica, MA) equipped with a CaptiveSpray nanoBooster ion source. The ^{12}C-/^{13}C-labeled mixtures were injected onto a Thermo Scientific Acclaim PepMap RSLC C18 column (75 μm × 150 mm, 2 μm particle size) (Sunnyvale, CA) via an Acclaim PepMap 100 trap column (75 μm × 20 mm, 3 μm particle size). The LC−MS conditions used are shown in Note S1.

Data Analysis. The raw LC−MS data were converted to the .csv file using Bruker Data Analysis software. The ^{12}C-/^{13}C-labeled metabolites were detected as peak pairs. We used ^{13}C-labeling to create the internal standard of a metabolite in the pooled sample for each ^{12}C-labeled metabolite in a sample. Since the same ^{13}C-labeled pool was added to individual ^{12}C-labeled samples and we measured the peak ratio of the ^{12}C-labeled metabolite versus ^{13}C-labeled metabolite, any signal variations due to the matrix effect, ion suppression effect, sample loss, instrumental drift, and so forth can be compensated, resulting in accurate relative quantification. The peak pairs were extracted and peak pair ratios were calculated by IsoMS Pro (Nova Medical Testing, Edmonton, Alberta).[24] Metabolite identification was carried out using the reported three-tier identification method.[26] The data were autoscaled (mean-centered and divided by the standard deviation of each variable) before the univariate and multivariate analyses were performed by IsoMS Pro.

https://dx.doi.org/10.1021/acs.analchem.0c04508
Anal. Chem. 2021, 93, 3418−3425

RESULTS AND DISCUSSION

LC-FLD Setting. The conjugated structure of the dansyl group makes it a good fluorochrome, and its fluorescent property has been used for quantifying amines.[27] The dansyl-labeled compounds emit green fluorescence at ~500 nm with UV excitation. However, a byproduct, dansyl hydroxyl (DnsOH), is produced during labeling, which interferes with the quantification of dansyl-labeled metabolites. Fortunately, DnsOH and dansyl-labeled metabolites can be separated on a C18 column using a simple step gradient.[11] The hydrophilic DnsOH elutes out using an aqueous solution, while dansyl-labeled metabolites elute out using an organic solvent. The separation was shown to be complete using fast-gradient LC–MS, instead of LC-UV.[28] To optimize the step gradient for LC-FLD, three different flow rates, 0.45, 0.55, and 0.65 mL/min, were compared (Figure S2); 0.45 mL/min was selected as an optimal flow rate. The excitation wavelength of LC-FLD was then optimized to maximize the fluorescence signals (Figure S3). Among the three wavelengths tested (227, 250, and 338 nm), 250 nm was selected for excitation and 520 nm was selected for emission detection. Other detector parameters were also optimized to further enhance the signal intensity, including the detector gain (Figure S4). The detector gain was set at 18 in this study. The sample injection volume was optimized to be 1 μL. With this low volume injection, sample consumption for LC-FLD was minimized.

Calibration Curve of Standards. The purpose of sample normalization is to equalize the concentration of the starting materials for all the samples. In the absence of a metabolome standard, accurate measurement of the total concentration of metabolites in a sample is not possible. However, to equalize sample concentrations, we only need to find a quantifier that functions as a surrogate of the total concentration of a sample.[9] The measured value of the quantifier may be different from the true total concentration of metabolites; however, the difference is a proportional constant. Based on the values of the quantifier, we can either dilute or concentrate a sample to make all samples to have the same concentration. In LC-FLD, the quantifier is the total concentration of all eluted dansyl-labeled metabolites in a sample that is determined using a calibration curve of dansyl-labeled amino-acid standards (Dns-AAS). We chose amino acids as they are readily available and are usually present in many different types of metabolome samples with relatively high concentrations. We used the mixture of 18 amino acid standards from Sigma-Aldrich directly without adjusting each amino acid concentration to that in a sample or considering mono- and multidansyl-group attachment to an amino acid, as the objective was not to determine the absolute total concentration of all metabolites.

Figure 1A shows the overlaid chromatograms of Dns-AAS at different concentrations. The peak eluted in 0.5–1.3 min was from Dns-OH, and the peaks eluted between 2.3 and 4 min were from dansyl-labeled metabolites. The peak areas of Dns-AAS were plotted as a function of concentration to establish a calibration curve (Figure 1B). As Figure 1B shows, a nonlinear region between 0.12 and 0.98 mM in a labeled solution of 21 μL is noticeable, mainly due to signal saturation. However, detection of high concentration is not a concern, as for concentrations of above 0.12 mM, the LC-UV method can be used for sample normalization. For LC-FLD, the linear range is from 2 to 120 μM, as shown in Figure 1C, with a linear correlation R^2 = 0.9993.

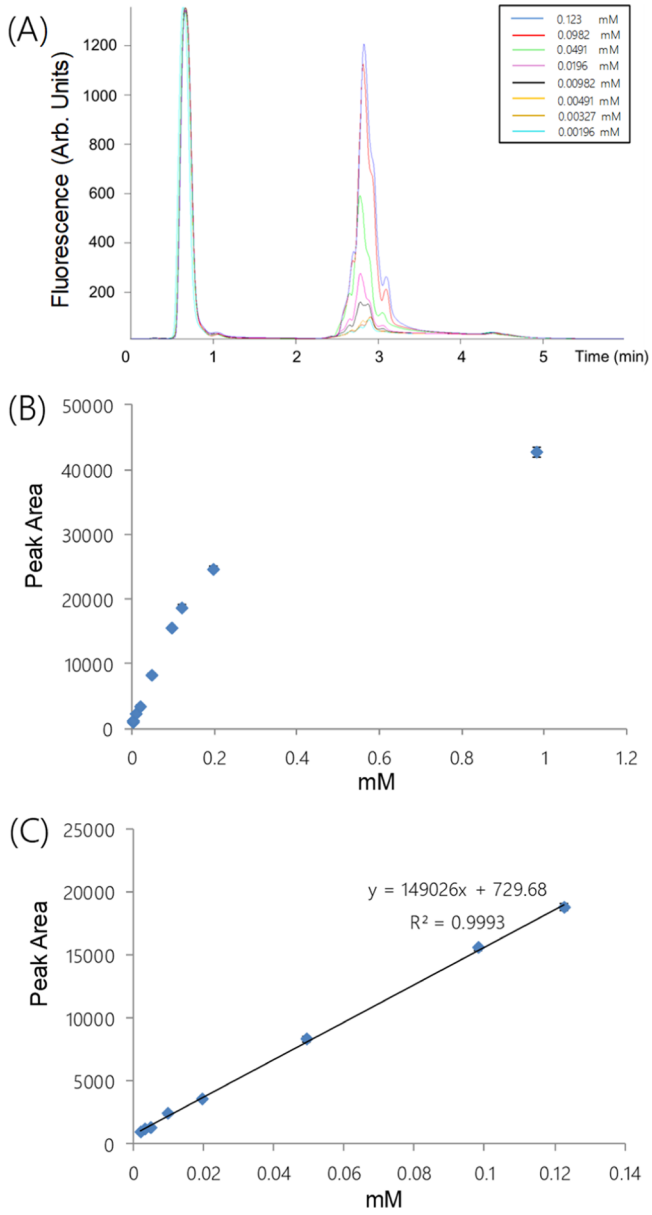

Figure 1. (A) Overlaid LC-FLD chromatograms of dansyl-labeled amino acid standards. (B) Peak areas of labeled amino acids as a function of concentration. (C) Calibration curve of labeled amino acids showing the linear region useful for LC-FLD-based sample normalization. The concentrations in the *x*-axis are based on the total volume of AAS after labeling (i.e., 21 μL).

Calibration Curve of Cell Lysates. To determine the range of cell numbers that the LC-FLD method can apply for sample normalization, we established a calibration curve of labeled cell lysates. In this case, 10^5 MCF-7 cells were lysed, extracted, diluted by 10-, 20-, 50-, 100-, 200-, 500-, and 1000-fold, which is equivalent to lysates of 10,000, 5000, 2000, 1000, 500, 200, and 100 cells, respectively, and then labeled using DnsCl. Triplicate injections of 1 μL labeled lysates were performed. Figure 2A shows the overlaid chromatograms. The peak profiles of labeled cell lysates are similar to those of Dns-AAS. The chromatographic peaks of labeled lysates look smoother, which can be attributed to the fact that the lysates contain many more different types of metabolites than AAS, creating more overlapped peaks.

https://dx.doi.org/10.1021/acs.analchem.0c04508
Anal. Chem. 2021, 93, 3418–3425

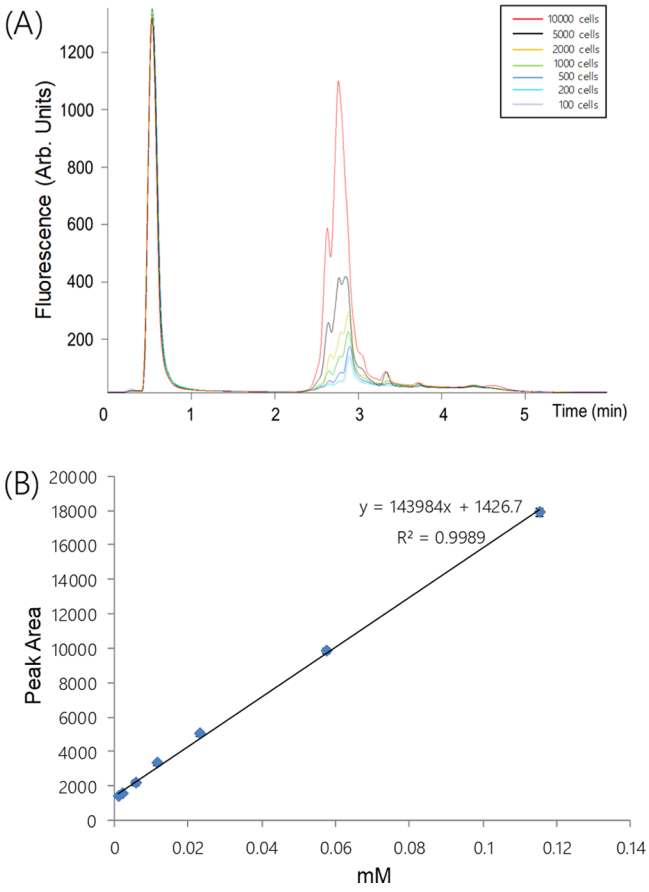

Figure 2. (A) Overlaid LC-FLD chromatograms of dansyl-labeled cell lysates. (B) Calibration curve of labeled cell lysates. The concentrations in the *x*-axis are based on the total volume of samples after labeling (i.e., 21 μL).

The total concentration of the labeled metabolites from cells was determined using the Dns-AAS calibration curve (Figure 1C). The measured concentrations of the labeled lysates at different numbers of cells are shown in Table S1. The calibration curve is shown in Figure 2B with good linearity (R^2 = 0.9989). Moreover, the slope of the calibration curve from the cell lysates (143984) is very similar to the slope of the Dns-AAS curve (149026), indicating that the overall fluorescence signal response from labeled cell lysates is similar to that of Dns-AAS. The intercepts on the *Y*-axis in Figures 1C and 2B are different, due to difference matrices of AAS and cell lysates. Thus, the calibration curve of Dns-AAS can be used for quantifying the total concentration of labeled metabolites in cell lysates relative to the Dns-AAS amount.

However, the calibration curve, shown in Figure 2B, does not reflect any sample loss during cell lysis and subsequent handling of the lysates from small numbers of cells because each diluted sample was prepared from a lysate of a large number of cells, that is, 10^5 cells. For a large number of cells, sample loss due to metabolite adsorption to the container wells may be negligible, compared to the total amount of sample. However, for small numbers of cells, metabolite adsorption may lose all or a large fraction of the analytes. Therefore, we can use a calibration curve to gauge any sample loss in working with small numbers of cells. For instance, if we assume that 500 cells are used as the real starting material and they are prepared perfectly (i.e., all cells are lyzed, all metabolites are extracted and labeled, and there is no sample loss before injection into LC-FLD), the total concentration of labeled metabolites should be 9.8 ± 1.0 μM, according to Figure 2B and Table S1. Any concentration departure from this value would suggest sample loss (see below).

Quantification of Labeled Lysates from Small Numbers of Cells. To quantify metabolites of small numbers of cells (not a diluted lysate of a larger number of cells), different numbers of cells were counted and aliquoted into separate vials. They were lysed, extracted, labeled, and analyzed by LC-FLD with triplicate injections. The total concentration of labeled metabolites in each sample was calculated using the calibration curve in Figure 2B. Note that we used the calibration curve of cell lysates for sample normalization, not the Dns-AAS calibration curve. For a different cell type (e.g., HeLa cells), a different calibration curve can be established for normalizing the samples of the given cell type. The concentration results are shown in Table S2. The total concentration of labeled metabolites found in an actual cell lysate was generally lower than that of the corresponding diluted lysate. For instance, the total concentration in actual 5000-cell lysates was found to be 52.0 ± 0.5 μM, which was lower than 61.0 ± 1.2 μM found in the equivalent 5000-cell diluted lysates. In the case of using 500 cells as the starting material, the total concentration of the labeled lysate was 6.9 ± 0.2, not 9.8 ± 1.0 μM. These reduced concentrations reflected sample loss when handling small numbers of cells.

Comparison of measured concentrations of actual lysates and diluted lysates also indicates that, for lower numbers of cells, the percentage of sample loss is higher. From Table S2, the measured concentrations of labeled metabolites in 100- and 200-cell lysates are no longer proportionally changed, in comparison to the concentration change from 500-cell to 200-cell lysates (i.e., 1.83-fold decrease from 200-cell to 100-cell lysates vs 1.64-fold decrease from 500-cell to 200-cell lysates). It is clear that a more severe sample loss was encountered when 100 cells were handled, compared to handling 200 or 500 cells. Therefore, the LC-FLD method is difficult to differentiate 100- and 200-cell lysates, suggesting a sample normalization limit of down to 200 cells. We note that lowering the detection limit of LC-FLD should be achievable using a more sensitive detection system such as a capillary column separation with a laser-induced FLD.[29] However, considering that the current method of CIL nanoLC−MS does not provide high-coverage metabolome analysis from a starting material of 200 cells or less,[22] we did not pursue any further to improve the LC-FLD detection limit; the current system and setup are adequate for our purpose of high-coverage metabolome profiling of 500 or more cells. Future work of developing more sensitive sample normalization methods needs to be carried out in parallel with the development of more sensitive metabolome analysis methods.

LC-FLD Applications in LC−MS Metabolomics. Many metabolomics application areas would benefit greatly from the use of a small amount of starting materials for metabolome analysis. Taking cellular metabolomics as an example, the benefits of using small numbers of cells are numerous, including reducing cost and time in large-scale cell-based testing of drug candidates, monitoring dynamics of cellular responses during different growth phases with and without a stimulant, analyzing few cells procured from tissues, studying circulating tumor cells isolated from biofluids, and so forth. In these applications, cell counting, a possible option for normalizing samples,[9] may not be doable or sufficiently accurate when the cell number is very small (<10^5 cells/mL).[30,31] We could not find any report of using

https://dx.doi.org/10.1021/acs.analchem.0c04508
Anal. Chem. 2021, 93, 3418−3425

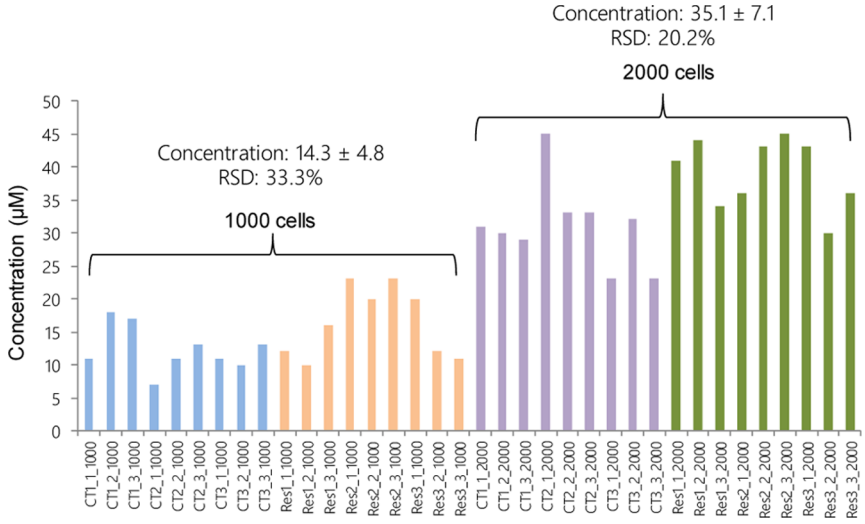

Figure 3. Bar graph showing the total metabolite concentrations determined by dansyl-labeling LC-FLD in different samples. The final volume of labeled lysates was 21 μL for each sample.

protein amount measurement to normalize samples for analyzing very few cells. We also do not know if protein amounts have any correlation with the metabolite amounts in the cell extracts. More importantly, direct measurement of metabolites is preferred, as any metabolite loss during the sample handling of small numbers of cells cannot be gauged by protein measurement from the cells.

Using nanoLC−MS, we have previously demonstrated the relative quantification of thousands of metabolites using a starting material of as low as 500 cells.[22] However, the LC-UV normalization method is not sufficiently sensitive to be compatible with this few-cell metabolomics workflow. In LC-UV, 5 μL of labeled lysates with a minimum concentration of 20 μM is required for injection into the column to measure the total concentration of labeled metabolites. In the optimized sample workflow for handling small numbers of cells, the final volume of labeled lysates is 21 μL. In other words, the LC-UV method can only quantify the total concentration of labeled metabolites in >2000-cell lysates, while still consuming ∼25% of the sample. With the development of LC-FLD for sample normalization, we can now complete the workflow for quantitative metabolome analysis of down to 500 cells, as described below.

Metabolomics of Small Numbers of MCF-7 Cells. To illustrate the workflow and its performance, we analyzed MCF-7 cells with and without the treatment of resveratrol, an antioxidant and potential anticancer compound.[32] Biological triplicate experiments were performed for each group. For each biological replicate sample, we performed experimental triplicate analysis. A hemocytometer was used to count the harvested cells. For each biological replicate, we took three aliquots that would contain about 1000 cells per sample calculated from the cell density and the aliquot volume. We took three additional aliquots with each containing about 2000 cells. Each individual sample was lysed, extracted, and labeled using ^{12}C-DnsCl. A pooled sample was also generated and labeled using ^{13}C-DnsCl. The labeled lysates were injected into LC-FLD for quantification. Figure 3 shows the quantification results from the experimental triplicate of biological triplicate samples, while Table S3 lists the concentrations of individual samples.

As Figure 3 shows, concentration varies for replicate samples, due to imprecision in cell counting and aliquoting of small numbers of cells, as well as variations in sample loss during the sample workup leading to the analysis. The concentration of labeled lysates of the 2000-cell samples ranges from 22.7 to 45.2 μM (a 2.0-fold difference) with an average concentration of 35.1 μM (Table S3) and a relative standard deviation (RSD) of 20.2%. For the 1000-cell samples, the labeled lysate concentration ranges from 7.10 to 23.2 μM (a 3.3-fold difference) with an average concentration of 14.3 μM (Table S3) and an RSD of 33.3%. Using the peak area values and the calibration curve shown in Figure S5, we can determine the equivalent number of cells in each sample. For the 1000-cell samples, the cell number ranges from 617 to 2017 cells. For the 2000-cell samples, the cell number ranges from 1969 to 3926 cells. Apparently, the initial cell numbers (1000 cells or 2000 cells) determined using a hemocytometer were not accurate. This is in agreement with a recent study that showed a good accuracy of cell counting (<7% error) at a low limit of ∼10^5 cells/mL using a hemocytometer, flow cytometer, Invitrogen cell counter, or smartphone cell counter.[30] However, an error of 46% was observed when counting cells from a solution of 5×10^4 cells/mL.[30]

It is clear that we need to normalize samples of small numbers of cells in order to accurately determine the concentration differences of individual metabolites in these samples. The normalization factor (NF), defined as (total concentration of individual sample)/(total concentration of pooled sample), for each labeled sample is shown in the last column of Table S3. The concentration of the labeled pool is 21.0 μM. As an example, the total concentration of labeled lysates of the sample, CT1_1_1000, one of the replicates of the 1000-cell samples, is 11.4 μM. The NF is 11.4/21.0 or 0.54. If equal volumes were used for mixing this ^{12}C-labled sample with the ^{13}C-labeled pool, the ^{12}C-labeled metabolite signals would be expected to be 0.54-fold of the ^{13}C-labeled metabolite signals. Thus, by multiplying a peak ratio in the LC-FLD-normalized dataset to a NF, we can produce a calculated unnormalized dataset.

Figure 4A shows the PCA 3-dimensional score plot of the metabolome data of these samples obtained by injecting the same amount of individual 1:1 ^{12}C-/^{13}C-mixtures, while Figure 4B shows the PLS-DA plot. The injection amount was chosen based on the lowest concentration (i.e., 7.1 μM) among all the labeled samples in 21 μL. This solution corresponded to a lysate of about 500 cells. For each sample, 1 μL of the 21 μL-labeled

https://dx.doi.org/10.1021/acs.analchem.0c04508
Anal. Chem. 2021, 93, 3418−3425

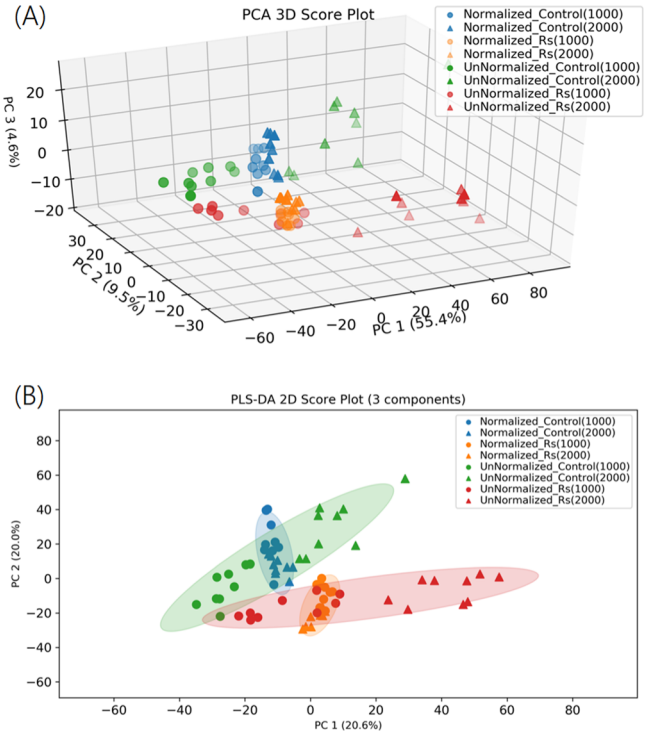

Figure 4. (A) PCA and (B) PLS-DA plots of the normalized and unnormalized metabolome data.

sample was consumed for LC-FLD quantification. The remaining solution of all individual samples with concentrations of >7.1 μM was diluted to be 7.1 μM. A 20 μL aliquot of the ^{12}C-labeled sample was taken to mix with an equal amount (i.e., 142 pmol) of the ^{13}C-labeled pool. The ^{12}C-/^{13}C-mixture was dried down and then redissolved in 7 μL of 9:1 (v/v) water/ACN. Five microliters of the mixture was injected into nanoLC−MS for metabolome analysis.

As Figure 4 shows, there are a total of eight subgroups. Of particularly interest is the comparison of the resveratrol treatment group and the control group, from which we can determine the significantly changed metabolites caused by resveratrol treatment. In the unnormalized dataset, both PCA and PLS-DA plots show the spread of the data points within the treatment or control group. Since the concentration range of the 1000-cell samples is very different from that of the 2000-cell samples, without normalization to the same concentration, these two subgroups of samples are well separated in the unnormalized samples. In contrast, the intragroup data points are more tightly clustered in the normalized dataset. In total, 1909 peak pairs were detected, and 78.8% of them could be identified or matched to different tiers of libraries.[26] Among them, 94 peak pairs were positively identified by searching against the dansyl standard library (Tier 1) using accurate mass and retention time information. A total of 159 peak pairs could be putatively identified with high confidence using a Linked ID library (Tier 2) that contains accurate mass and predicted retention time information of pathway-related metabolites. A total of 75, 618, and 558 peak pairs could be mass-matched by searching against zero-, one-, and two-reaction MCID libraries (Tier 3), respectively. The identified or matched peak pairs are listed in Table S4.

We used univariate analysis to determine the significantly changed metabolites in the resveratrol treatment group vs the control group. Figure 5A,B shows the volcano plots of LC-FLD-normalized and unnormalized datasets, respectively. The cutoff

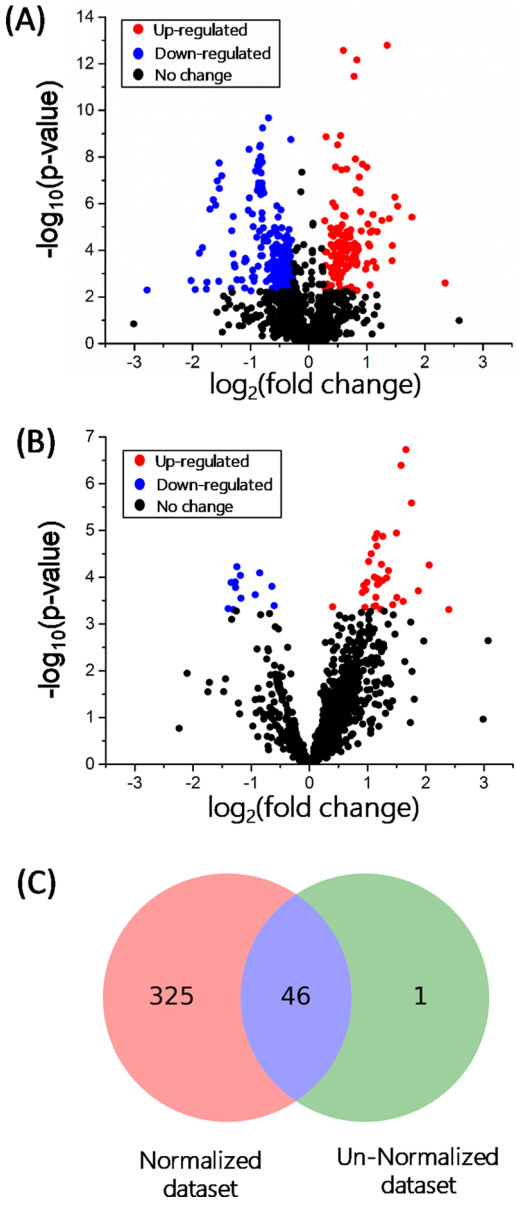

Figure 5. Volcano plots of (A) normalized and (B) unnormalized metabolome data. The same FDR-adjusted p-value (Storey's q-value) of <0.01 was used as the threshold, leading to different nonadjusted p-value thresholds shown in (A,B). (C) Venn diagram of the number of significant metabolites found from the normalized and unnormalized datasets.

value used was a fold-change of more than 1.2 or less than 0.83 with the false discovery rate (FDR)-adjusted p-value of less than 0.01. For the normalized samples, 130 metabolites have significantly increased concentrations in the treatment group and 241 metabolites have significantly decreased concentrations. For the unnormalized samples, there are 35 metabolites with increased concentrations and 12 metabolites with decreased concentrations. Figure 5C shows the Venn diagram comparing the numbers of significant metabolites found in the normalized and unnormalized datasets. There are 46 significant metabolites in common, and 325 unique metabolites are found in the normalized dataset, but only one unique metabolite is

https://dx.doi.org/10.1021/acs.analchem.0c04508
Anal. Chem. 2021, 93, 3418−3425

found in the unnormalized dataset (Tables S5 and S6). It is clear that sample normalization is critical for measuring concentration changes between two different groups of samples. The study of the biological significance of the significantly changed metabolites is beyond the scope of this work.

CONCLUSIONS

We have developed a highly sensitive LC-FLD method for metabolome sample normalization. This method is useful for measuring the dansyl labeled metabolites in a 21 μL solution in the range of 2−120 μM. With 1 μL injection, LC-FLD consumes 4.8% of the labeled sample. Above 120 μM, the previously reported LC-UV method can be used. The LC-FLD method should be generally useful for quantifying metabolome samples of limited amounts, such as in few-cell metabolomics. As an example, the lysates of small numbers of MCF-7 cells from the resveratrol-treated group and the control group were quantified and normalized by LC-FLD, followed by CIL nanoLC−MS analysis, using a starting material of down to 500 cells. Comparison of the normalized and unnormalized datasets showed a significant improvement in data quality after performing LC-FLD normalization. We envisage the use of this LC-FLD method for quantification of metabolites in small volumes of serum or plasma, exosomes, sweat, tear drop, and so forth, as part of the integrated workflow in CIL LC−MS-based platform for high-coverage quantitative metabolomics. We note that, for metabolome analysis of large amounts of samples, LC-UV should be used as it is more convenient to analyze high-concentration samples without the risk of saturating the detector of LC-FLD. While the application example demonstrated in this work is for cellular metabolomics, for analyzing tissue samples, one may estimate the number of cells present in a tissue to determine the minimum size of tissue for LC-FLD analysis. For other types of samples with limited amounts, we hope to demonstrate the utility of LC-FLD in future application-oriented studies.

ASSOCIATED CONTENT

Supporting Information

The Supporting Information is available free of charge at https://pubs.acs.org/doi/10.1021/acs.analchem.0c04508.

Notes for the experiments, figures for study design and data analysis, and tables for metabolite quantification results (PDF)

List of matched or identified metabolites (XLSX)

List of significant metabolites found in normalized data (XLSX)

List of significant metabolites found in un-normalized data (XLSX)

AUTHOR INFORMATION

Corresponding Author

Liang Li − *Department of Chemistry, University of Alberta, Edmonton, Alberta T6G 2G2, Canada;* orcid.org/0000-0002-9347-2108; Email: Liang.Li@ualberta.ca

Authors

Xian Luo − *Department of Chemistry, University of Alberta, Edmonton, Alberta T6G 2G2, Canada*

Yiman Wu − *Department of Chemistry, University of Alberta, Edmonton, Alberta T6G 2G2, Canada*

Complete contact information is available at: https://pubs.acs.org/10.1021/acs.analchem.0c04508

Author Contributions

†X.L. and Y.W. contributed equally.

Notes

The authors declare no competing financial interest.

ACKNOWLEDGMENTS

This work was supported by the Natural Sciences and Engineering Research Council of Canada, Canada Research Chairs, Canada Foundation for Innovation, Genome Canada, and Alberta Innovates.

REFERENCES

(1) Pezzatti, J.; Boccard, J.; Codesido, S.; Gagnebin, Y.; Joshi, A.; Picard, D.; González-Ruiz, V.; Rudaz, S. *Anal. Chim. Acta* **2020**, *1105*, 28.

(2) Zhao, S.; Li, L. *TrAC, Trends Anal. Chem.* **2020**, *131*, 115988.

(3) Kruve, A. *Anal. Chem.* **2020**, *92*, 4691−4699.

(4) Shen, K.; Wang, L.; He, Q.; Jin, Z.; Chen, W.; Sun, C.; Pan, Y. *Anal. Chem.* **2020**, *92*, 1763−1769.

(5) Zheng, S.-J.; Zheng, J.; Xiong, C.-F.; Xiao, H.-M.; Liu, S.-J.; Feng, Y.-Q. *Anal. Chem.* **2020**, *92*, 2043−2051.

(6) Hao, L.; Zhu, Y.; Wei, P.; Johnson, J.; Buchberger, A.; Frost, D.; Kao, W. J.; Li, L. *Anal. Chim. Acta* **2019**, *1088*, 99−106.

(7) Barrientos, R. C.; Zhang, Q. *Anal. Chem.* **2019**, *91*, 9673−9681.

(8) Jia, S.; Xu, T.; Huan, T.; Chong, M.; Liu, M.; Fang, W.; Fang, M. *Environ. Sci. Technol.* **2019**, *53*, 5445−5453.

(9) Wu, Y.; Li, L. *J. Chromatogr. A* **2016**, *1430*, 80.

(10) Zhou, R.; Li, L. *J. Proteomics* **2015**, *118*, 130.

(11) Wu, Y.; Li, L. *Anal. Chem.* **2012**, *84*, 10723−10731.

(12) Chen, D.; Han, W.; Huan, T.; Li, L.; Li, L. *Anal. Chem.* **2020**, *92*, 9265−9272.

(13) Dahabiyeh, L. A.; Malkawi, A. K.; Wang, X.; Colak, D.; Mujamammi, A. H.; Sabi, E. M.; Li, L.; Dasouki, M.; Rahman, A. M. A. *Metabolites* **2020**, *10*, 42.

(14) Chen, D.; Yu, J.; Zhang, Z.; Su, X.; Li, L.; Li, L. *Anal. Chem.* **2019**, *91*, 4958−4963.

(15) Mung, D.; Li, L. *J. Food Drug Anal.* **2019**, *27*, 565−574.

(16) Hsu, C.-W.; Chen, Y.-T.; Hsieh, Y.-J.; Chang, K.-P.; Hsueh, P.-C.; Chen, T.-W.; Yu, J.-S.; Chang, Y.-S.; Li, L.; Wu, C.-C. *Anal. Chim. Acta* **2019**, *1050*, 113−122.

(17) Adeyemi, J. A.; Harmon, D. L.; Compart, D. M. P.; Ogunade, I. M. *J. Anim. Sci.* **2019**, *97*, 4657−4667.

(18) Liao, H.-W.; Rubakhin, S. S.; Philip, M. C.; Sweedler, J. V. *Anal. Chim. Acta* **2020**, *1118*, 36−43.

(19) Liu, R.; Sun, M.; Zhang, G.; Lan, Y.; Yang, Z. *Anal. Chim. Acta* **2019**, *1092*, 42−48.

(20) Huang, T.; Armbruster, M.; Lee, R.; Hui, D. S.; Edwards, J. L. *J. Chromatogr. A* **2018**, *1567*, 219−225.

(21) Luo, X.; An, M.; Cuneo, K. C.; Lubman, D. M.; Li, L. *Anal. Chem.* **2018**, *90*, 8314−8319.

(22) Luo, X.; Li, L. *Anal. Chem.* **2017**, *89*, 11664−11671.

(23) Guo, K.; Li, L. *Anal. Chem.* **2009**, *81*, 3919−3932.

(24) Zhou, R.; Tseng, C.-L.; Huan, T.; Li, L. *Anal. Chem.* **2014**, *86*, 4675−4679.

(25) Han, W.; Li, L. *Metabolomics* **2015**, *11*, 1733.

(26) Zhao, S.; Li, H.; Han, W.; Chan, W.; Li, L. *Anal. Chem.* **2019**, *91*, 12108−12115.

(27) Herrero, A.; Sanllorente, S.; Reguera, C.; Ortiz, M. C.; Sarabia, L. A. *Anal. Chim. Acta* **2016**, *945*, 31−38.

(28) Xu, W.; Chen, D.; Wang, N.; Zhang, T.; Zhou, R.; Huan, T.; Lu, Y.; Su, X.; Xie, Q.; Li, L.; Li, L. *Anal. Chem.* **2015**, *87*, 829.

(29) Novotny, M. V. *J. Chromatogr. A* **2017**, *1523*, 3−16.

(30) Kang, W.; Huang, H.; Cai, M.; Li, Y.; Hou, W.; Yun, F.; Wu, X.; Xue, L.; Wang, S.; Liu, F. *Anal. Chim. Acta* **2019**, *1077*, 216−224.

(31) Fagète, S.; Steimer, C.; Girod, P.-A. *J. Biotechnol.* **2019**, *305*, 23−26.
(32) Ferraz da Costa, D. C.; Rangel, L. P.; Duarte da Cunha Martins-Dinis, M. M.; da Silva Ferretti, G. D.; Ferreira, V. F.; Silva, J. L. *Molecules* **2020**, *25*, 893.

https://dx.doi.org/10.1021/acs.analchem.0c04508
Anal. Chem. 2021, 93, 3418−3425